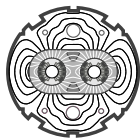


EUROPEAN ORGANIZATION FOR NUCLEAR RESEARCH
European Laboratory for Particle Physics*Large Hadron Collider Project***LHC Project Report 9****Measurement of the primary photodesorption yield at 4.2 K, 77 K and room temperature in a quasi-closed geometry**

V. Baglin

Abstract

In the context of the Large Hadron Collider project, the normal incidence photodesorption yield of neutral gases from a stainless steel surface has been measured at 4.2 K, 77 K and room temperature. The yields were measured using a synchrotron radiation photon beam with a critical energy of 45.3 eV, which is very near that to be expected in the LHC. It has been shown that the primary photodesorption yield decrease with decreasing temperature. The gases desorbed were H₂, CH₄, CO and CO₂. At 4.2 K and 77 K the H₂O primary photodesorption yield was practically zero. At room temperature the primary photodesorption yields were $5 \cdot 10^{-4}$, $1.6 \cdot 10^{-5}$, $2.5 \cdot 10^{-4}$ and $2.2 \cdot 10^{-4}$ molecules photon⁻¹ respectively for H₂, CH₄, CO and CO₂. At 77 K the primary photodesorption yields of H₂, CH₄, CO and CO₂ were reduced by factors of 2, 4, 17 and 32 respectively with respect to room temperature. At 4.2 K, these corresponding reduction factors were 14, 20, 42 and 31.

LHC-VAC

Administrative Secretariat
LHC Division
CERN
CH - 1211 Geneva 23
Switzerland

Geneva 7 June 1996

Measurement of the primary photodesorption yield at 4.2 K, 77 K and room temperature in a quasi-closed geometry

V. Baglin *CERN, 1211 Geneva 23, Switzerland.*

In the context of the Large Hadron Collider project, the normal incidence photodesorption yield of neutral gases from a stainless steel surface has been measured at 4.2 K, 77 K and room temperature. The yields were measured using a synchrotron radiation photon beam with a critical energy of 45.3 eV, which is very near that to be expected in the LHC. It has been shown that the primary photodesorption yield decrease with decreasing temperature. The gases desorbed were H₂, CH₄, CO and CO₂. At 4.2 K and 77 K the H₂O primary photodesorption yield was practically zero. At room temperature the primary photodesorption yields were $5 \cdot 10^{-4}$, $1.6 \cdot 10^{-5}$, $2.5 \cdot 10^{-4}$ and $2.2 \cdot 10^{-4}$ molecules photon⁻¹ respectively for H₂, CH₄, CO and CO₂. At 77 K the primary photodesorption yields of H₂, CH₄, CO and CO₂ were reduced by factors of 2, 4, 17 and 32 respectively with respect to room temperature. At 4.2 K, these corresponding reduction factors were 14, 20, 42 and 31.

I. INTRODUCTION

In the Large Hadron Collider (LHC) the synchrotron radiation photons emitted in the bending magnet by the 7.0 TeV proton beam will hit the beam screen, which will operate at a temperature between 5 K and 20 K, and desorb neutral gases which, in turn, will contribute to the limitation of the beam lifetime [1]. The pressure inside the beam pipe will be essentially dominated by this photodesorption since the thermal desorption of all gases except He will be very small at this temperature. The partial pressure due to the vapour pressure of H₂ will remain low provided the surface coverage stays well below a monolayer and the temperature is much less than 20 K. Nevertheless, perforations will be provided in the beam screen to enable the desorbed gas to be pumped onto the 1.9 K cold bore located behind, thus limiting the pressure inside the beam screen.

In order to be able to predict the behaviour of the vacuum system when subjected to photon bombardment, it is necessary to know the primary photodesorption yields at the temperatures of operation of the beam screen. For this purpose, the CERN Electron Positron Accumulator (EPA) synchrotron radiation beam line used previously for measurement of photodesorption yields at room temperature [2], has been modified to measure these yields at cryogenic temperature.

I. EXPERIMENTAL DETAILS

The system layout is shown schematically in Fig 1 and the measuring apparatus has already been described in ref. [2]. A 316 LN stainless steel cylinder, chemically cleaned, of diameter 45 mm and 155 mm long is built into a cryostat containing either liquid He or liquid N₂. This sample tube can therefore be completely immersed in He at 4.2 K or N₂ at 77 K, thus ensuring a well defined temperature. In this geometry, the photons directly illuminate the end face of the cylinder at normal incidence over a geometrical area of 7.3 cm².

In order to simulate as close as possible the actual conditions in the LHC the sample tube was not baked.

To be able to detect all photodesorbed gases, a warm Cu tube, of diameter 36 mm and 350 mm long, connects the room temperature part of the system to the entry of the sample tube. With the sample tube immersed in He at 4.2 K, and thermal screening at 77 K around it, the measured temperature of the warm

tube remains under all conditions above 283 K. This temperature prevents parasitic cryosorbing on the warm tube and allows a direct measurement of the molecules photodesorbed from the cold target.

Total and partial pressures were measured with a calibrated Bayert-Alpert (B.A.) type vacuum gauge and a calibrated quadrupole gas analyser used with a SEM. The system was pumped through a conductance located at room temperature with a calculated value of 72.5 l s^{-1} for N_2 . The pressure behind the conductance was always at least one order of magnitude lower than in the measurement part. With the calibrated gauges, this allowed the number of molecules passing through the known conductance to be measured.

The beam of synchrotron radiation, which also passed through the conductance, was square in section ($27 \times 27 \text{ mm}$ at the end face of the target) and had a critical energy of 45.3 eV which is close to the 44.1 eV of the LHC at its nominal energy of 7.0 TeV. The square collimator for the radiation was dimensioned such that photons down to 4.2 eV were transmitted with negligible attenuation. At 45.3 eV critical energy the maximum power deposited in the sample was 90 mW and the photon flux used for computation was $4.1 \cdot 10^{16} \text{ photons s}^{-1}$ and didn't take into account the low energy part of the photon spectrum attenuated by the collimator.

All data taking was done on a computer every 4 seconds using LabVIEW software.

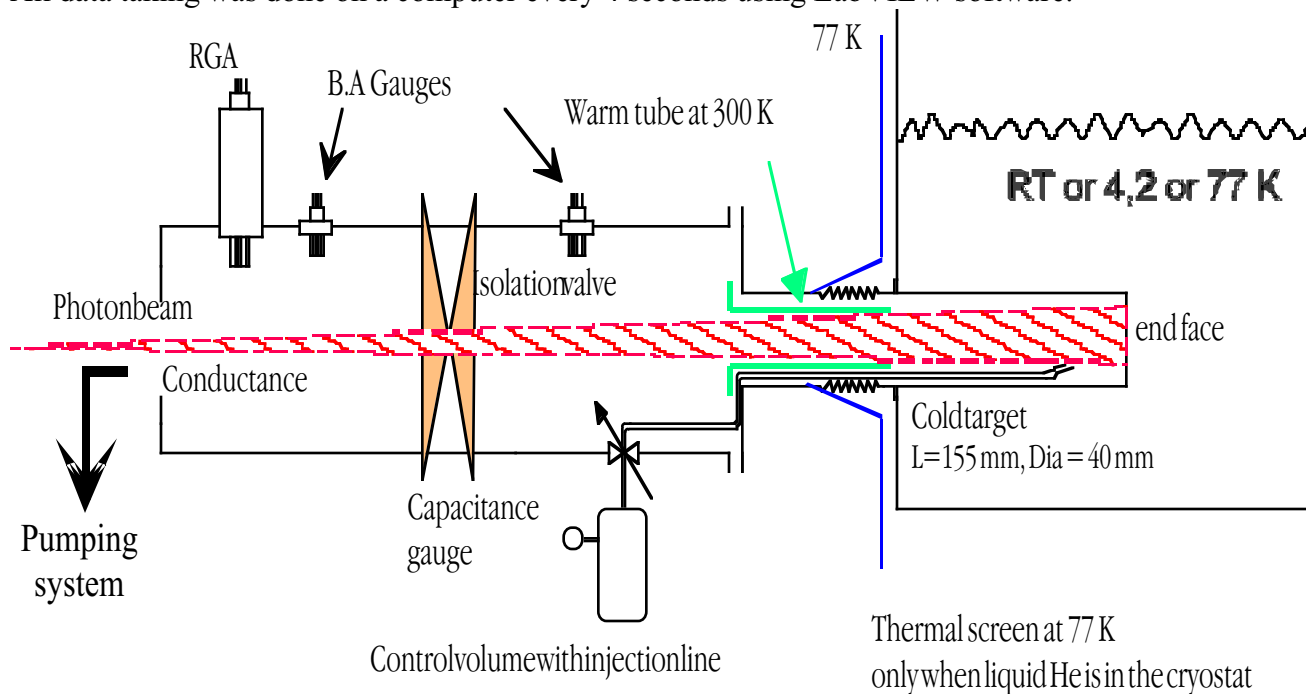


Fig 1. Experimental layout

I. SIMULATION OF H_2 PHOTODESORPTION

In order to simulate the photodesorption of H_2 and verify the behaviour of the apparatus, H_2 gas was injected directly into the sample tube at 4.2 K via a small capillary line as shown in Fig 1.

The capillary was connected to a reservoir of known volume (1.075 litre) filled with H_2 to a pressure of about 1 Torr, measured with a capacitance gauge. By recording the decrease in pressure with time in the reservoir the flux of H_2 injected (Torr l s^{-1}) can be measured. Simply measuring the change in pressure gives the total quantity injected.

With the isolation valve closed, therefore no external pumping, and liquid He in the cryostat, the H_2 isotherm at 4.2 K was measured point by point by injecting known quantities of H_2 and measuring the equilibrium pressure after each injection on the B.A. gauge located at room temperature. The isotherm was also measured by continuously injecting H_2 at a rate of $2 \cdot 10^{-5} \text{ Torr l s}^{-1}$ ($0.9 \cdot 10^{-3} \text{ monolayer s}^{-1}$ on a geometrical sample area of 235 cm^2 where 1 monolayer is assumed to be $3 \cdot 10^{15} \text{ molecules cm}^{-2}$) a rate

which is here equivalent to a primary photodesorption yield of $1.6 \cdot 10^2 \text{ H}_2 \text{ photon}^{-1}$. The results are shown in

Fig 2 where it can be seen that there is a good correspondence between the two methods. This shows that if the Knudsen relationship is valid in the point by point method, it is also valid in the continuous method with a good confidence, also at least for a primary photodesorption yield below $1.6 \cdot 10^2 \text{ H}_2 \text{ photon}^{-1}$. The measured value of the saturated vapour pressure for H_2 of $6 \cdot 10^{-6}$ Torr in equilibrium at 300 K equals, assuming simple thermal transpiration, $1.6 \cdot 10^{12} \text{ H}_2 \text{ cm}^{-3}$ at 4.2 K and agrees well with that measured by other workers [3,4,5]. But the value obtained for the surface coverage at the “knee” cannot be compared because the end face of the sample was electroeroded and could have had a higher surface roughness.

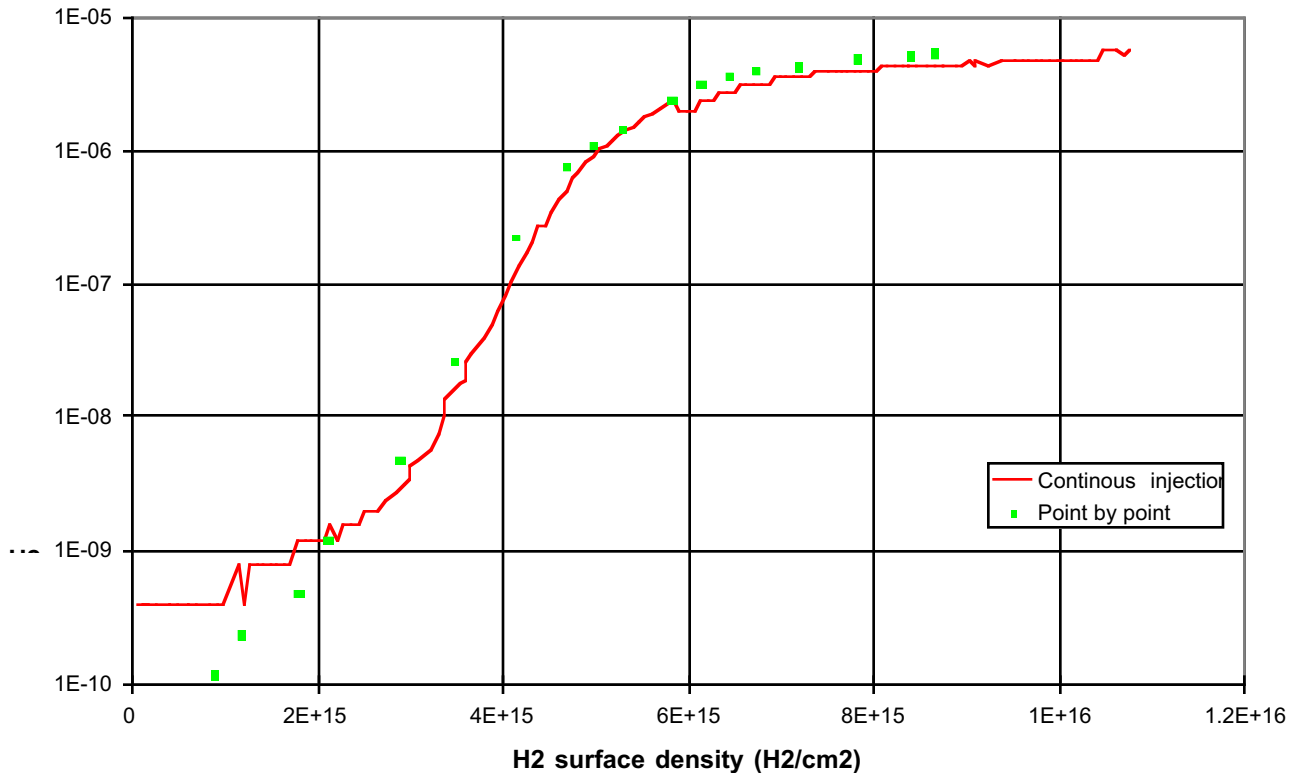


Fig 2. H_2 isotherm at 4.2 K for continuous and point by point injection

In a second step, with the isolation valve open and therefore external pumping, H_2 was injected into the sample tube at several different but constant flux levels.

When a constant flux of H_2 is injected into the 4.2 K sample tube some gas is physisorbed and the surface coverage gradually increases, and some H_2 is pumped out through the conductance. With increasing surface coverage, the H_2 vapour pressure increases and the quantity pumped out through the conductance increases. An equilibrium will be reached when the quantity of gas pumped by the cold surface is balanced by the gas leaving the surface due to the increased thermal evaporation (vapour pressure). In this situation the effective pumping speed of the 4.2 K surface is zero and all the injected gas is pumped through the conductance. Therefore a series of increasing H_2 fluxes gives rise to a series of increasing ΔP 's. However for higher fluxes, when the 4.2 K surface reaches its saturated vapour pressure it will continue to pump and reduced increases in ΔP takes place.

This is illustrated in Fig 3 where it can be seen that, starting at a base pressure of $1 \cdot 10^{-10}$ Torr, the pressure measured at room temperature immediately increases to about $2 \cdot 10^{-10}$ Torr when the H_2 injection is started and then slowly increases due to the increasing surface coverage. The equilibrium is clearly observed and new higher equilibrium pressures with larger injected fluxes are also evident. The effect of saturation at the highest fluxes is also demonstrated. Note that the full saturated vapour pressure is not measured in this situation due to the pumping of the system via the conductance.

The lack of H_2 net pumping speed at equilibrium was demonstrated as follows. With the isolation valve open, a known quantity of H_2 was injected at a constant flux into the 4.2 K sample tube until equilibrium was obtained and continued well after. The tube was then slowly warmed up and the number of H_2 molecules released and pumped through the conductance was measured by integrating the pressure times the conductance with respect to time. It was found that the number of molecules desorbed corresponded within 2.5 % to that injected only up to the time required to attain the equilibrium.

If Q (Torr l s $^{-1}$) is the flux of H_2 gas, C is the conductance (l s $^{-1}$) and ΔP is the increase in H_2 partial pressure at equilibrium then

$$Q = C \Delta P \quad (1)$$

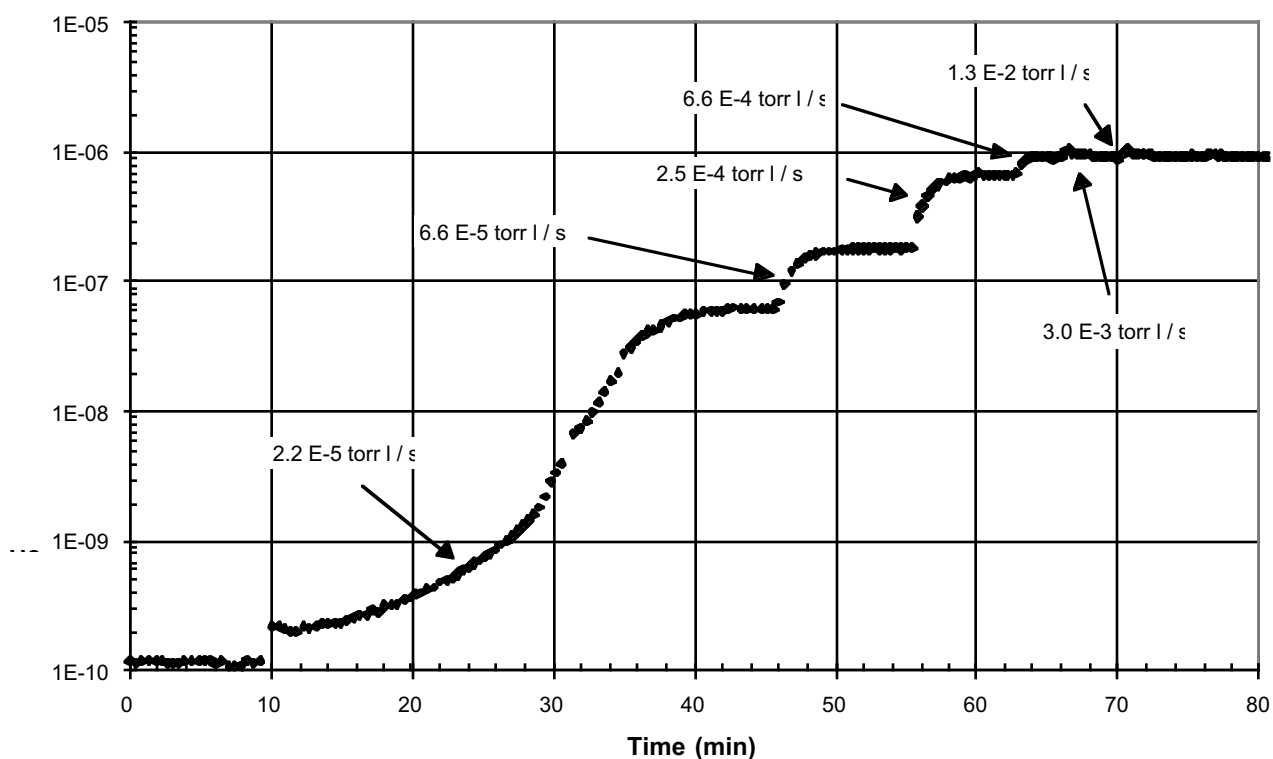


Fig 3. Typical result of a dynamic H_2 isotherm with different injection fluxes

By plotting the equilibrium pressure versus injecting flux, the value of the conductance may be obtained. The results are shown in Fig 4 where the linear increase of the equilibrium pressure with flux at low flux is evident. Also shown is the plateau, in theory a straight line with nearly zero slope, obtained when the surface is saturated. The level of this plateau is less than the $6 \cdot 10^{-6}$ Torr saturation pressure quoted previously since it is reduced due to the pumping through the conductance. The value of the conductance obtained from the slope of the straight line agrees to within 3% with the value obtained by calculation from the dimensions thus giving a useful cross check and confidence in the predicted behaviour of the system.

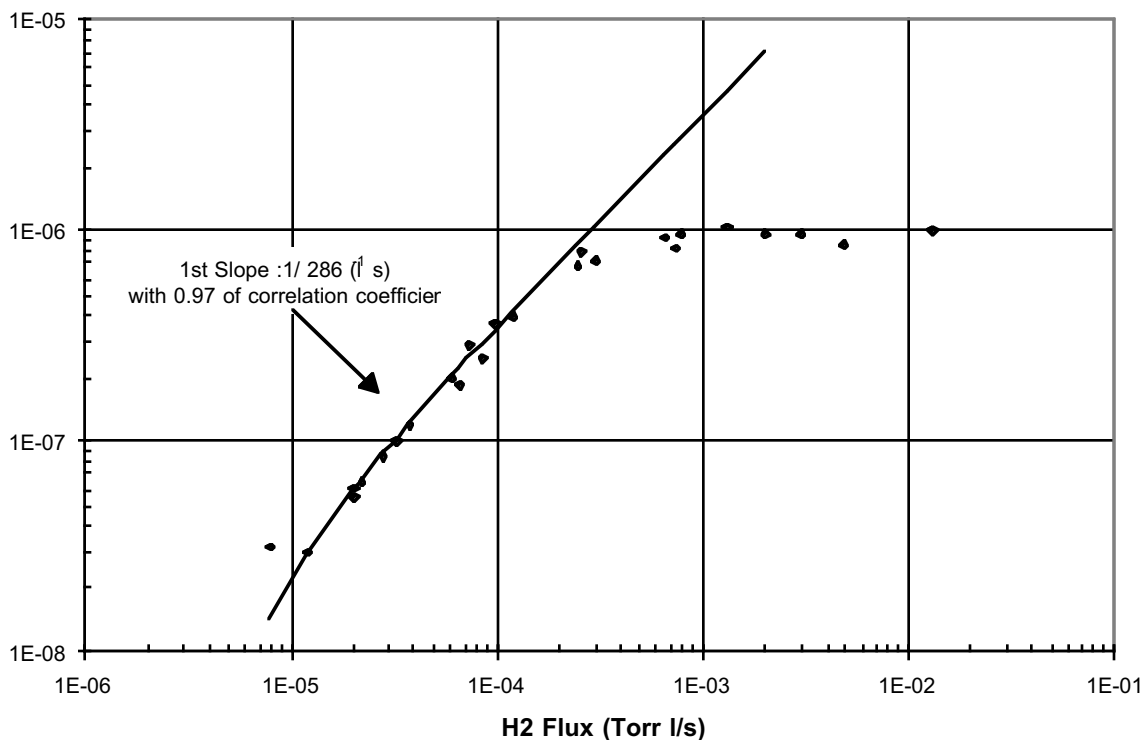


Fig 4. Equilibrium pressures versus injected flux during a dynamic isotherm measurement

I. PHOTODESORPTION OF H₂ AT 4.2 K

When the sample tube is irradiated by photons, this situation is somewhat more complicated in that there are two desorption yields, namely primary and recycling (usually called secondary) [5]. The primary photodesorption is due to tightly bound gas molecules which are desorbed by the photons from the near oxide surface. Only molecules desorbed by the primary effect constitute a source of gas. The recycling photodesorption is due to photodesorption of weakly bound gas molecules physisorbed (cryopumped) on the cold surface. The H₂ recycling yield can be much larger than primary yield and it increases with surface coverage [6].

Under photon bombardment, the photodesorbed H₂ is pumped partly by the cold surface and partly through the conductance, as in the case of the injection of H₂ gas. However, in addition to the pressure increase by thermal desorption from increasing surface coverage there is a pressure increase due to the recycling effect. In practice, the two effects act together and the system behaves qualitatively as in the injection situation reaching an equilibrium pressure when the effective pumping speed of the cold surface is zero.

In our experimental setup, only a part of the cold sample is directly irradiated, the other remaining part accumulates the desorbed gas. As the surface coverage on the non-irradiated surface grows, an equilibrium will be also reached due, now, to the H₂ isotherm alone and hence at a higher surface coverage than that for the irradiated part.

In equilibrium (the variation with time of pressure and surface coverage is zero) or quasi-equilibrium (the variation of pressure and surface coverage is slow in time and the time scale is long compared to the molecular transit time across the tube diameter), an amount equivalent to all the primary desorbed H₂ escapes through the conductance and can therefore be measured by the gauge at room temperature giving a reliable value for the photodesorption yield at low temperature.

I. PHOTODESORPTION OF OTHER GASES AT 4.2 K AND 77 K

Contrary to H_2 , at 4.2 K the other gases desorbed by photons such as CH_4 , CO and CO_2 have negligible vapour pressures even at large surface coverages. But their behaviour under photon bombardment is expected to be similar to that of H_2 in that there is an equilibrium situation where the pressure increase with coverage is due only to the recycling effect. Thus, the low temperature photodesorption yield for these gases could also be measured by the same method.

However, since in our experiment only the end face of the sample tube is directly illuminated by photons the neighbouring cold surfaces can pump indefinitely the desorbed gas. This lowers the pressure increase observed at room temperature and hence the calculated desorption yield by an unknown amount for which it is difficult to correct. However, this problem can be avoided by allowing the cold surface to slowly warm up and the number of physisorbed molecules pumped by the conductance can be added to the number of molecules desorbed during irradiation in order to calculate an average primary photodesorption yield (total number of desorbed molecules/total number of photons).

On the other hand, at 77 K, the vapour pressures of H_2 , CH_4 , CO and CO_2 are large enough to allow an equilibrium or quasi-equilibrium, even on the non irradiated surface, as in the case of H_2 at 4.2 K. Again, the primary photodesorption yields could be measured by the same method.

I. MATHEMATICAL DESCRIPTION OF THE SIMULATION

The above simulation can be simply described on the basis of the equations describing the rate of change of the pressure P in a volume V and the surface density θ on the surface A developed in ref. [5].

$$\begin{cases} V \frac{dP}{dt} = Q + \frac{1}{G} \frac{A}{\tau(\theta)} \theta - S P - C P \\ A \frac{d\theta}{dt} = -\frac{A}{\tau(\theta)} \theta + G S P \end{cases} \quad (2)$$

where Q is the gas injection flux, A is the surface area, S is the pumping speed of the cold surface, C is the value of the conductance, $\tau(\theta)$ is the sojourn time for probability of the thermal desorption of the physisorbed molecules and G is a constant converting Torr l to molecules.

The second term in the top equation describes the gas leaving the surface due to the thermal evaporation (vapour pressure) and the last two terms are the gas pumped by the cold surface and through the conductance respectively.

In the second equation, the change in surface density is determined by the gas leaving the surface due to the vapour pressure (first term) and the gas cryosorbed on the surface (second term).

When the surface coverage is constant ($d\theta/dt = 0$), the rate of the thermal evaporation is exactly balanced by the rate of the physisorption of molecules and the effective pumping speed is zero. Since the surface coverage is constant the pressure stabilises at this value ($dP/dt = 0$) and is simply given by :

$$P_{Eq} = \frac{Q}{C} \quad (3)$$

where C equals the value of the conductance. Note that this relation, is only valid for an injected flux giving an equilibrium pressure less than the saturated vapour pressure. In the case of saturation, the equilibrium pressure is defined by the saturated vapour pressure, the injecting flux, the cold surface pumping speed and the pumping provided by the conductance. The P over Q slope is now defined by two parallel pumps : the cold surface pumping and the external pumping. As this sum is big, this slope is nearly zero and appears as a plateau.

I. PHOTODESORPTION RESULTS

A. Calculation of desorption yields

It must be emphasised that the photodesorption yield η can only be determined in the present system when an equilibrium or quasi-equilibrium pressure P_{Eq} is reached and the effective pumping speed of the cold surface is zero. In this case the expression for η can be obtained from a system of equations similar to the above [5]:

$$\begin{cases} V \frac{dn}{dt} = \eta \dot{\Gamma} + \eta' \dot{\Gamma} - \frac{A}{\tau(\theta)} \theta - S n - C n \\ A \frac{d\theta}{dt} = - \eta' \dot{\Gamma} - \frac{A}{\tau(\theta)} \theta + S n \end{cases} \quad (4)$$

Where n is the molecular density, θ the surface density of physisorbed molecules, V the tube volume, A the tube area, $\dot{\Gamma}$ the photon flux, η and η' primary and recycling photodesorption yields and with the same meaning for other symbols.

When the rate of recycling molecules plus the rate of thermal evaporated molecules due to vapour pressure is exactly balanced by the rate of pumping molecules on the cold surface, the surface coverage is constant ($d\theta/dt = 0$) and the pressure stabilise ($dP/dt = 0$). The system is in equilibrium, it behaves as if it were a room temperature photodesorption experiment, the derivatives vanish and we have :

$$\eta = \frac{G C P_{Eq}}{\dot{\Gamma}} \quad (5)$$

where C is the pumping speed of the conductance ($l s^{-1}$), $\dot{\Gamma}$ is the photon flux ($photons s^{-1}$) and G is a constant converting Torr l to molecules. Note firstly that, in the equilibrium situation, the calculation of the primary photodesorption yield does not require a knowledge of the sticking coefficient for the gases on the surface. Secondly, the Knudsen relationship does not have to be applied because the pressure is measured at the conductance located at room temperature.

A. Short irradiation runs at 4.2 K and 77 K

Several photodesorption runs at different critical energies were carried out in a quasi-equilibrium situation i.e. the variation of pressure and surface coverage is slow in time. Before cooling the cryostat the desorption yield was first measured at room temperature. Then measurement of primary photodesorption yields were done at 4.2 K or 77 K. All measurements at room temperature were carried out with the lowest photon dose possible to minimise any cleaning effect of the surface.

One way to check for equilibrium or quasi-equilibrium is to vary the photon flux while giving a small overall dose in order to minimise the cleaning effect thus ensuring a constant primary photodesorption yield. This was done on a dedicated run at 4.2 K with 10 different beam currents varying over one order of magnitude. As shown in Fig 5, this gives a linear dependence of the measured partial pressure versus the current, with a correlation coefficient ranging from 0.91 to 0.95 for all gases, demonstrating that the measured primary photodesorption yields are indeed constant. This quasi-equilibrium could be obtained thanks to the reflected photons and photoelectrons.

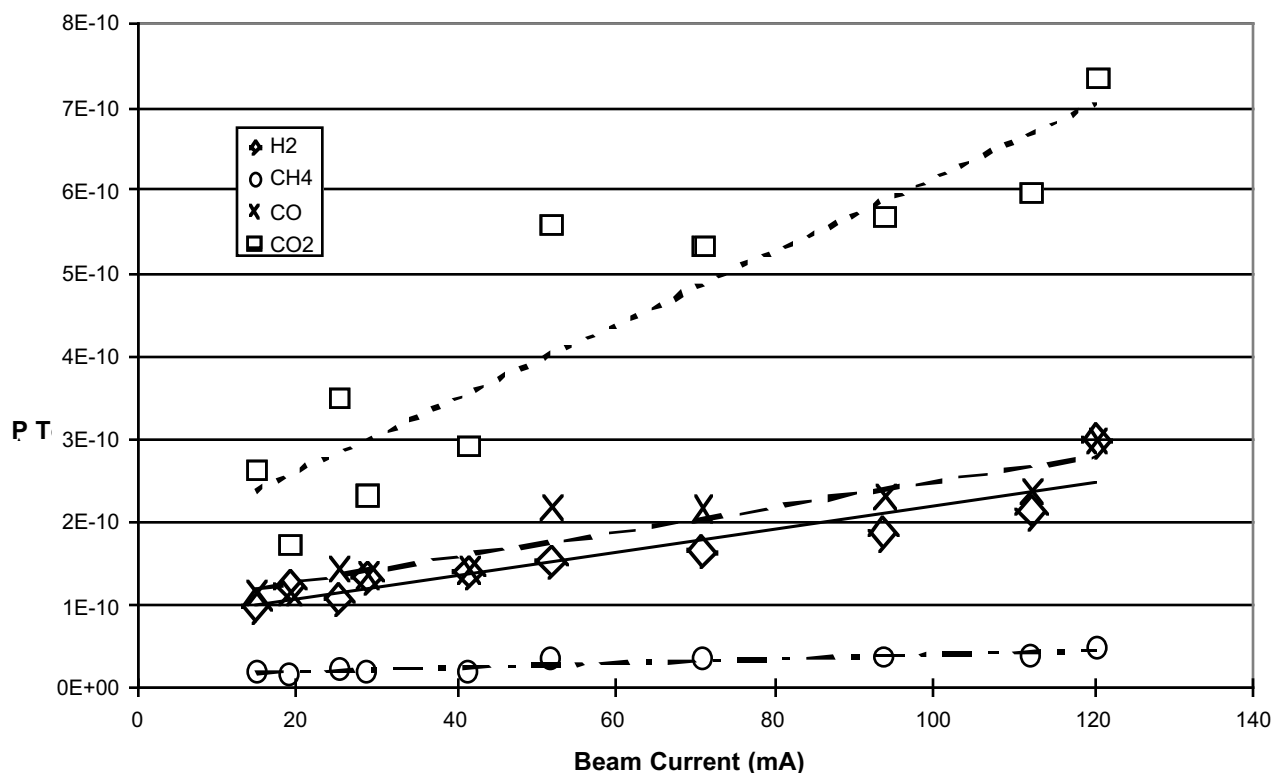


Fig 5. Equilibrium pressure versus beam current at 4.2 K.

Another way to check for equilibrium or quasi-equilibrium is to produce a non-equilibrium situation and see if the partial pressure goes towards the usual equilibrium value. This was done on several experiments dedicated to measure the recycling yields by injecting, before irradiation, a known amount of gas on the cold target. When subjected to short irradiation, a pressure bump, due to recycling, was seen and, after a while, the partial pressure reached the usual equilibrium value as if there were no gas on the surface. This shows that we were in equilibrium or quasi-equilibrium.

Moreover, by allowing the sample to warm up slowly after the 4.2 K photodesorption experiment, we can estimate the number of molecules of each species condensed on the surface by integrating the partial pressures measured at room temperature with respect to time and multiplying by the appropriate value for the conductance. This number, added to the total number of molecules passing through the pumping conductance during the irradiation and divided by the total number of incident photons gives an average primary photodesorption yield. This average primary photodesorption yield is in agreement with the above calculated primary photodesorption yield at 4.2 K in quasi-equilibrium within a factor of 2.

A. Long irradiation run at 4.2 K

During this irradiation experiment an equilibrium situation was reached. A total dose of $1.0 \cdot 10^{21}$ photons cm^{-2} was accumulated on the end face of the target (15.9 cm^2).

As shown in Fig 6, at the start of irradiation the H_2 pressure, measured at room temperature, immediately increases from its base value of $2 \cdot 10^{-10}$ Torr to $4.2 \cdot 10^{-10}$ Torr. The rapid increase is followed by a slow increase partly due to the recycling effect and partly due to vapour pressure change. The vertically aligned points are the decrease in pressure when stopping the irradiation for 2-3 minutes. Finally, after 21 h ($2 \cdot 10^{20}$ photons cm^{-2}), an equilibrium pressure of about $8.5 \cdot 10^{-10}$ Torr was obtained.

Thus the primary desorption yield η for H_2 may be calculated using equation (5) above with $P_{eq} = 6.5 \cdot 10^{-10}$ Torr.

Also evident, from this experiment, is the increasing of the base pressure when the irradiation is off which may be due to the increase of the H_2 surface coverage and hence vapour pressure, on the cold, non-irradiated areas of the sample.

A similar slow increase to a less extent, may be due to the recycling effect, was also observed for the other gas species but their behaviour was not so evident as for H_2 and needs more investigation. For this other gas species, the situation is more complicated because the non-irradiated areas of the cold surface pump indefinitely the desorbed gas without reaching any equilibrium.

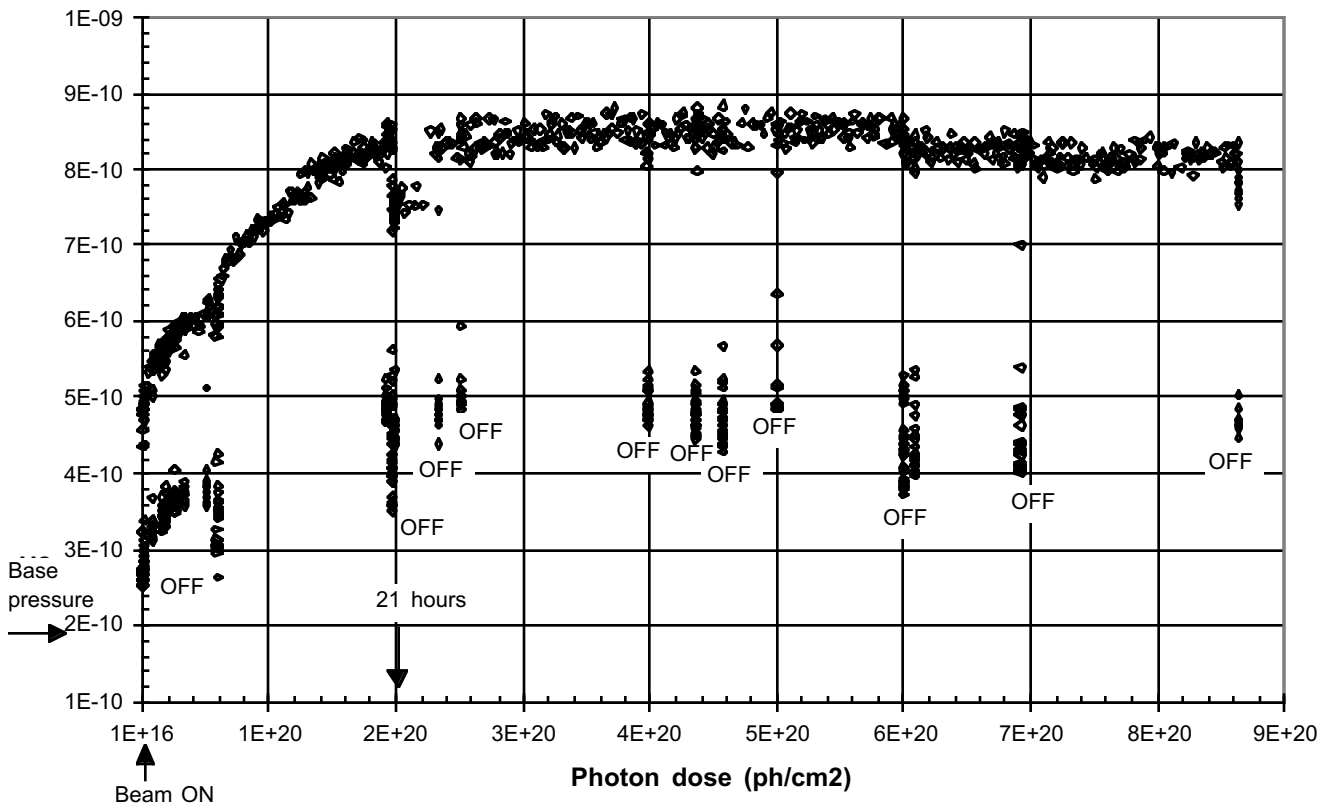


Fig 6. H_2 partial pressure during irradiation run

A. Long irradiation run at 77 K

During this period, a total dose of $1.14 \cdot 10^{21}$ photons cm^{-2} was accumulated on the end face of the target. Whereas a similar behaviour for CO_2 at 77 K as H_2 at 4.2 K was expected, no increase in partial pressure due to vapour pressure and/or recycling were recorded. As this increase in partial pressure is proportional to the pumping speed of the cold surface, this suggests that the CO_2 sticking coefficient at 77 K is relatively small compared to the H_2 one at 4.2 K.

Nevertheless, the average primary photodesorption yields measured were in agreement to within 50 % with the ones calculated during the short irradiation.

A. Primary photodesorption yields and variation with temperature

In Fig 7 below are presented two sets of measurements of the primary photodesorption yields at room temperature, at 77 K and at 4.2 K at a critical energy of 45.3 eV. The measurement were done after a long irradiation of the sample in order to prevent from any cleaning effect during the temperature tests. We

first took a measurement of the primary photodesorption yield at room temperature, cool down the cryostat at 77 K and took a second measurement. We let then the cryostat warming up and pumped for several days. Thirdly, we took another measurement at room temperature in order to verify that there were no cleaning effect. Last, we took a measurement at 4.2 K. The results were obtained in a quasi-equilibrium situation and calculated using equation (5). The results are also summarised in Table 1.

T (k)	H ₂	CH ₄	CO	CO ₂
RT	5.0 10 ⁻⁴	1.6 10 ⁻⁵	2.5 10 ⁻⁴	2.2 10 ⁻⁴
77	2.5 10 ⁻⁴	4.0 10 ⁻⁶	1.5 10 ⁻⁵	7.0 10 ⁻⁶
4.2	3.5 10 ⁻⁵	8.0 10 ⁻⁷	6.0 10 ⁻⁶	7.0 10 ⁻⁶
RT/77	2	4	17	31
RT/4.2	14	20	42	31

Table 1. Measured primary photodesorption yields (molecules/photon) at RT, 77 and 4.2 K on a stainless steel target at normal incidence at a critical energy of 45.3 eV.

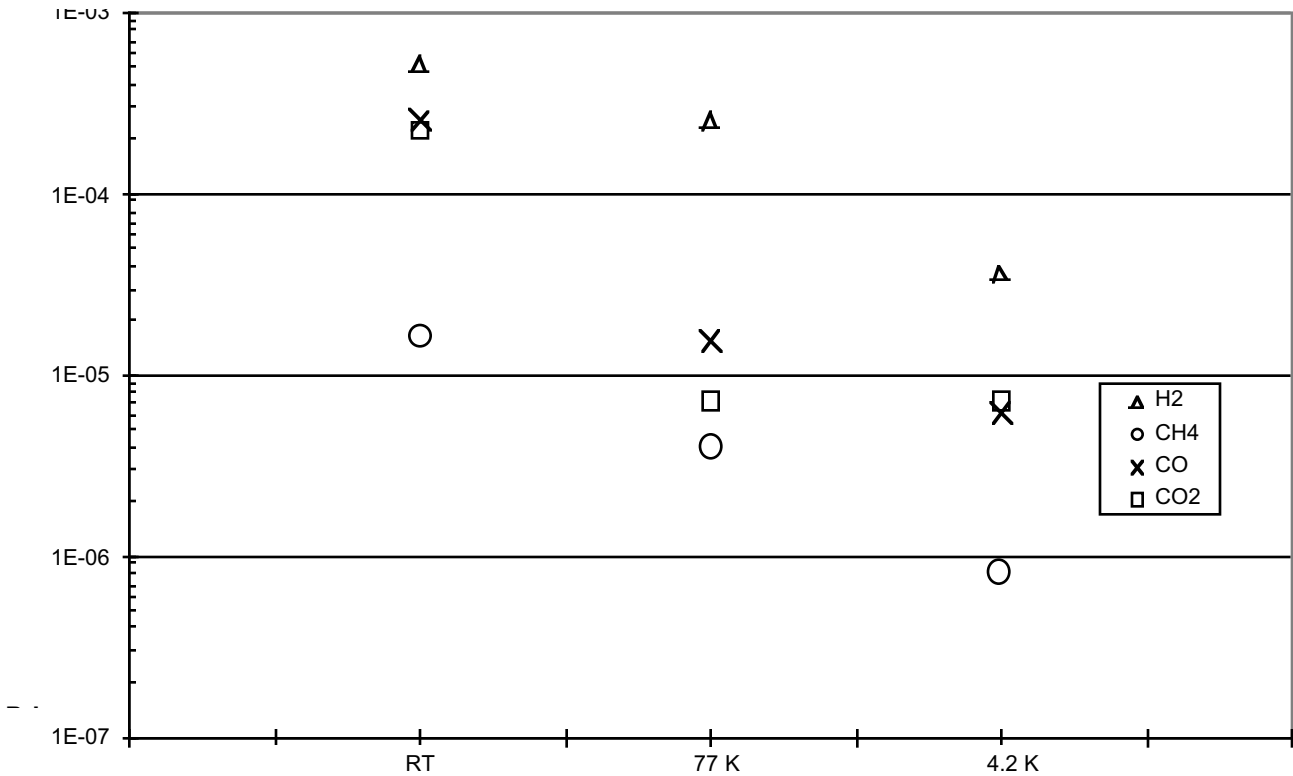


Fig 7. Primary photodesorption coefficient for a stainless steel surface at RT, 77 K and 4.2 K at a critical photon energy of 45.3 eV.

I. DISCUSSION-COMPARISON

The pressure measured at room temperature gives a yield (η_{Cold}) which represents the number of molecules per incident photon not pumped by the cold surface i.e. passing the conductance. Thus, if we assume, for argumentation and demonstration, that the primary photodesorption yields are independent of the temperature, we can compute the number N of monolayers pumped on the cold surface for a number n of incident photons :

$$N = \frac{n \cdot (\eta_{RT} - \eta_{Cold})}{A \cdot \theta_m} \quad (6)$$

where n is the number of incident photons, A is the cold surface area (235 cm^2), θ_m is the monolayer coverage (taken to be equal to $3 \cdot 10^{15} \text{ molecules cm}^{-2}$ for all gases), $(\eta_{RT} - \eta_{Cold})$ represents the number of molecules pumped by the cold surface where η_{RT} and η_{Cold} are the primary photodesorption yields measured at room temperature and 77K or 4.2 K respectively. η_{RT} and η_{Cold} are taken from the Table 1. This calculation is independent of the state of the system i.e. equilibrium or not.

With our actual setup the maximum number of photons incident on the target was $1.8 \cdot 10^{22}$ and $1.6 \cdot 10^{22}$ photons at 77 K and 4.2 K respectively (Fig 6). The Table 2 below shows the results for the computed number of monolayers N .

T (k)	H ₂	CH ₄	CO	CO ₂
77	6.4	0.3	6.0	5.5
4.2	10.6	0.4	5.6	4.9

Table 2. Computed number of monolayers theoretically cryosorbed on the cold surface for primary photodesorption yields assumed to be independent of the temperature and equal to the room temperature values.

At 4.2 K, if the primary photodesorption yields were equal to its room temperature value, 10 monolayers of H₂ should have been condensed resulting in a high saturated vapour pressure! But no big increase in pressure due to vapour pressure was recorded with increasing photon dose. Also the theoretical numbers of monolayers condensed on the surface of the other gases CH₄, CO and CO₂ exceeded by far the number recovered during slow warm-up.

In addition, at 77 K we should have reached a relatively high pressure due to the vapour pressure for all the gases except perhaps CH₄ but no such high pressure were measured.

From these striking discrepancies, one must conclude that the primary photodesorption yields decrease with temperature.

This conclusion plus the current test, the average measurement and the expected behaviour of H₂ during long irradiation give us confidence in the behaviour and results of the primary photodesorption yield at different temperatures.

At 77K, compared to the yields at room temperature, the yields for CO and CO₂ are reduced by factors of 17 and 31 respectively. For H₂ and CH₄ the decrease is much less being 2 and 4 respectively.

At 4.2 K the decrease in the yields with respect to room temperature is somewhat more, 14 for H₂, 20 for CH₄ and 42 for CO and 31 for CO₂.

In ref. [7], the authors found a ratio of ~ 0.5 at 4.2 K. This discrepancy could be due to their open sample geometry without external pumping where an equilibrium pressure cannot be reached. There were also difficulties to distinguish the primary from the recycling photodesorption coefficient and interpret the data in their experiment. Thus the ratio could be overestimated because, as demonstrated later [6], the recycling photodesorption coefficient could be much larger than the primary photodesorption coefficient.

The results obtained at 77 K are in agreement with ref. [8] within a factor of three but are totally different with the estimated 4.2 K data in the same reference. Here, it has to be noted that these measurements were done with a simple beam tube i.e. with little external pumping, thus physisorption leads to a non equilibrium state, especially at 4.2 K, also within this setup the primary photodesorption coefficient cannot directly be measured.

In a later version, a beam screen with holes i.e. with external pumping was inserted in the same setup ref [5] allowing a direct measurement of the primary photodesorption. At 4.2 K the ratio is only given

for H₂ and CO and is 3. The discrepancy between our results could be due to the transmission probability through the beam screen hole set to 0.59 and to illumination at grazing angle.

Recently, this same setup was used to characterise a LHC beam screen prototype [9] and the results obtained at 77 K show the same order of reduction as ours.

I. CONCLUSION

Normal incidence primary photodesorption yields were measured in a quasi-closed geometry on a stainless steel surface at a critical energy of 45.3 eV. The value of the measured primary photodesorption yields was demonstrated to be correct when the effective pumping speed of the surface is zero. At this instant, an equilibrium or quasi-equilibrium pressure was reached where an equivalent amount of all the primary desorbed gas passed the measuring conductance. This zero effective pumping speed was obtained in our devices thanks to the external pumping. The LHC pressure behaviour will be the same thanks to the holes in the beam screen which provide external pumping.

Despite the fact that the measured pressure increase could be lowered for CH₄, CO and CO₂ at 4.2 K (see section 5) and hence the measured primary photodesorption yield, the measurement was cross-checked, and found to be in agreement within a factor of 2, by a measurement by the average method.

The results have shown that there is a decrease in the primary photodesorption yield measured at cryogenic temperature compared to room temperature. At 77 K the desorption yields of H₂, CH₄, CO and CO₂ were reduced by 2, 4, 17 and 31 respectively with respect to room temperature. At 4.2 K, these corresponding reduction factors were 14, 20, 42 and 31.

ACKNOWLEDGEMENTS

The author would like to thank Mr P. Cruikshank and Mr M. Karmarkar who designed the cryostat. He is also indebted to Mr J. M. Rieubland and Mr G. Ferlin for assistance in the cryogenic laboratory and for helium supplying and Dr J. P. Potier and his operating crew for running the EPA machine well out of its normal operating range. He would like also to thank Drs V. Anashin, R. Calder, O. Gröbner, O. Malyshev, A. Mathewson and W. Turner for their many critical and fruitful discussions on the subject and Mr A. Grillot for his support during mounting, developing and operating the experiment.

REFERENCES

- [1] The Large Hadron Collider, Conceptual Design Report, CERN/AC/95-05(LHC), 15 October, 1995.
- [2] Comparison of photodesorption yields using synchrotron radiation of low critical energies for stainless steel, copper, and electrodeposited copper surfaces, J. Gómez-Goñi, O. Gröbner, and A.G. Mathewson, *J. Vac. Sci. Technol. A* 12(4), 1714 Jul/Aug (1994).
- [3] Influence of thermal radiation on the vapor pressure of condensed hydrogen (and isotopes) between 2 and 4,5 K, C. Benvenuti, R. S. Calder and G. Passardi, *J. Vac. Sci. Technol. Vol. 13, No. 6*, 1172 (1976).
- [4] Adsorption isotherms of H₂, CH₄, CO and CO₂ on a copper plated stainless steel at 4.2 K, E. Wallén. CERN, LHC Project Report 5, 1996.
- [5] Cold beam tube photodesorption and related experiments for the Superconducting Super Collider Laboratory 20 TeV proton collider, V. V. Anashin, G. Derevyankin, V. G. Dudnikov, O. B. Malyshev, V. N. Osipov, C. L. Foerster, F. M. Jacobsen, M. W. Ruckman, M. Strongin, R. Kersevan, I. L. Maslennikov and W. C. Turner, *J. Vac. Sci. Technol. A* 12(4), 1663, Jul/Aug (1994).
- [6] Investigation of synchrotron radiation-induced photodesorption in cryosorbing quasiclosed geometry, V. V. Anashin, O. B. Malyshev, V. N. Osipov, I. L. Maslennikov and W. C. Turner, *J. Vac. Sci. Technol. A* 12(5), 2917, Sep/Oct (1994).
- [7] Photodesorption from copper-plated stainless steel at liquid-helium temperature and at room temperature, D. Bitinger, P. Limon, R.A. Rosenberg, *J. Vac. Sci. Technol. A* 7(1), 59 (1989).
- [8] Summary of recent photodesorption experiments at VEPP2M, V. Anashin, A. Evstigneev, O. Malyshev, V. Osipov, I. Maslennikov, W. Turner. SSCL-N-825, June 1993.

[9] Synchrotron radiation induced gas desorption from a prototype LHC beam screen at cryogenic temperature, R. Calder, O. Gröbner, A. G. Mathewson, V. V. Anashin, A. Dranichnikov and O. B. Malyshev. CERN AT/95-42 (VA) LHC project note 7, September 1995.